Journal of Alloys and Compounds 509 (2011) 1310–1313

Contents lists available at ScienceDirect

Journal of Alloys and Compounds

journal homepage: www.elsevier.com/locate/jallcom

The improvement of microwave properties for Co flakes after silica coating

Xu Yan*, Guozhi Chai, Desheng Xue

Key Lab for Magnetism and Magnetic Materials of the Ministry of Education, Lanzhou University, Tianshuinan Route 222#, Lanzhou 730000 730000, PR China

ARTICLE INFO

Article history:
Received 7 March 2010
Received in revised form 2 October 2010
Accepted 7 October 2010
Available online 16 October 2010

Keywords:
Nanostructures
Chemical synthesis
Magnetic measurements

ABSTRACT

Sub-micrometer cobalt flakes were successively fabricated by hydrazine reduction in aqueous solution, the flakes were coated with silica layers by the hydrolysis method. Their microwave and static magnetic properties were investigated. The silica coated cobalt flakes are characterized with high resonance frequency at 4 GHz, and the real part of permeability μ' were greatly improved when frequency was lower than resonance frequency. The improvement is ascribed to the suppression of eddy current loss after silica coating. The spectra of complex permeability were fitted with the Landau–Lifshitz–Gilbert equation and the resonance mode is proved to be the natural resonance mode.

1. Introduction

Magnetic core materials with low energy loss, high permeability and operating frequencies are crucial part in the development of high speed motor, generator, inductors, and current convectors as well as the further demands of miniaturization in power transformers [1–7]. For a long time, traditional soft ferrites materials (NiZn or Co_2Z ferrites, etc.) were the only choice for magnetic core materials in high frequency application [8–10], whereas their intrinsic magnetization is low and hard to be further increased, which seriously limits their applications in higher frequency [11]. Metal or alloy materials with high permeability and magnetization can be a better choice. However, serious energy loss caused by the eddy-current loss at high frequency deteriorates the high frequency magnetic properties. In order to decrease the eddy-current loss, metal materials are preferred to be fabricated as thin flakes with insulation coating [12], the ferromagnetic flakes with large shape anisotropy are able to exceed the Snoek's limit and show higher permeability in the GHz range [13,14]. In recent years, metal materials with insulation coating for high frequency application in GHz band have attracted considerable attentions. Basalt fiber/nickel core–shell heterostructures, CNTs/Fe and iron phosphate–silane composites have been prepared by various methods [15–17].

Zhao et al. have fabricated sub-micrometer laminated Fe/SiO_2 composites [12]; Zhang et al. prepared polymer composites consisting of aligned Fe flakes [18]. Though the magnetization and permeability of the composites are greatly enhanced, the resonance frequency is still lower than 1 GHz. To obtain a composite with higher resonance frequency, a material with higher magnetocrystalline anisotropy is required. It is known that the magnetocrystalline anisotropy of cobalt (*hcp* phase) is higher than that of iron [19], which could be used to fabricate nanocomposite with higher resonance frequency. In this paper, cobalt and silica coated cobalt flakes were prepared by hydrazine reduction in aqueous solution combined the hydrolysis method, and their microwave and static magnetic properties were investigated.

2. Experimental details

Cobalt flakes were prepared by hydrazine reduction in aqueous solution at 180 °C. A reaction solution was prepared by dissolving 0.002 mol $CoCl_2{\cdot}6H_2O$ and 0.073 g hexadecyl trimethyl ammonium bromide (CTAB) into 22 ml distilled water. Some amount of sodium hydroxide (NaOH) solution was added into the former solution with vigorous stirring and the dark brown suspension was formed gradually. Then 2.5 ml aqueous hydrazine ($N_2H_4{\cdot}H_2O$) with 85% concentration was added drop wise into the above suspension. The mixture was stirred vigorously until homogeneous and then transferred into a 50 ml steel autoclave. The clave was sealed and maintained at 180 °C for 3 h and then cooled naturally to the room temperature. The product was washed with distilled water and ethanol several times to remove the impurities and then dried at 40 °C. The product was named as sample 1.

0.5 g resulted powders were redispersed in 50 ml 2-propanol and sonicated for 20 min, 3 ml tetraethoxysilane and 20 ml of a 25 vol.% NH_3 in H_2O solution were added to the above dispersion, and the mixture was vigorously stirred for 1 h to complete the hydrolysis reaction. By means of magnetic decantation, the product was separated from the supernatant solution. It was washed with ethanol for several times to remove any unreacted organic chemicals, and finally dried in a desiccator. The obtained composites were named as sample 2. Sample 3 was fabricated by similar process except for the mount of tetraethoxysilane increased to 10 ml.

The crystal structures of the cobalt flakes were analyzed by X-ray diffraction (XRD) on a Philips Panalytical X'pert diffractometer with CuKα radiation. The morphology of the samples was investigated by a Hitachi S-4800 field emission scanning electron microscope (SEM). The measurements of selected area electron diffraction (SAED) and energy disperse spectrum (EDS) were performed on a transmission electron microscope (TEM) (JIM-2010). The static magnetic properties of the samples were measured by a Lake Shore 7304 vibrating sample magnetometer (VSM). The

* Corresponding author.
E-mail address: yax03@lzu.cn (X. Yan).

0925-8388/$ – see front matter © 2010 Elsevier B.V. All rights reserved.
doi:10.1016/j.jallcom.2010.10.022

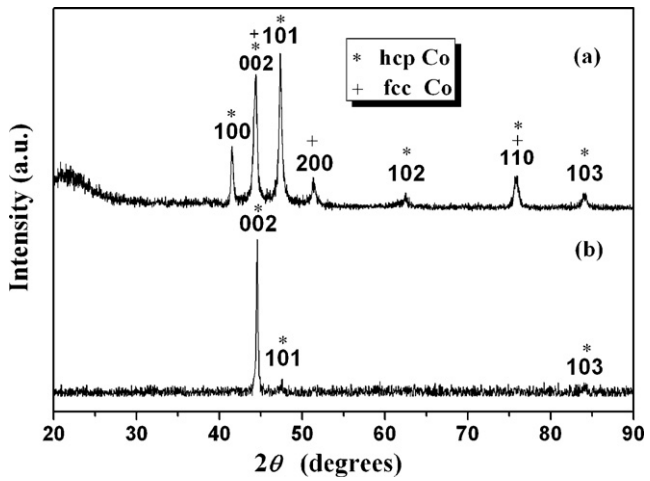

Fig. 1. X-ray diffraction spectrum of (a) sample 1 and (b) consolidated sample 3.

samples for microwave electromagnetic properties measurement were pressed into toroidal shape (Φ_{out} 7.00 mm, Φ_{in} 3.00 mm). The scattering parameters (S_{11}, S_{21}) were measured on the toroidal-shaped composites by a network analyzer (Agilent Technologies E8363B) in the range of 0.1–10 GHz. All of the measurements were performed at the room temperature.

3. Results and discussion

Fig. 1(a) shows the XRD spectrum of sample 1. Two cobalt phases can be observed, the major phase is *hcp* structure, and the other is *fcc* structure. Fig. 1(b) shows the XRD spectrum of consolidated sample 3. There is a (0 0 2) texture for *hcp* cobalt phase. The signal of silica was not detected.

SEM and TEM results show that the fabricated sample of Co is the flake shape. Fig. 2(a) shows that the diameter of flakes varied from 5–10 μm, and the thickness is around 160–190 nm. Fig. 2(b) shows the cobalt flakes coated with fine silica particles. The edge of a silica coating flake of sample 3 is presented in Fig. 2(c). The thickness of the coating is around 40–70 nm. In Fig. 2(d) and (c) a part of coated flake and corresponding selected area electron diffraction pattern are displayed, which exhibit sixfold symmetry with electron beam being along the ⟨0 0 1⟩ axis of *hcp* crystal structure. This means that the flakes are nearly single crystals and the growth of (0 0 1) plane is inhabited during the process of crystal growth. The selective absorption of the stabilizing agents (OH^-) on the close-packed planes of the *fcc* phase or *hcp* phase retards the growth perpendicular to the close packed planes, which leads to the formation of flake shape [20]. Selective absorption of the ligands onto the crystallographic planes is the key to control the shape of the nanoparticles [21]. The signal of silica coating is not observed in the SAED pattern, which indicates that the silica does not form a crystal structure. Fig. 2(f) shows the EDS pattern of sample 3 and the result shows the coexistence of Co, Si and O elements in this sample.

The mass ratio of cobalt in the composites can be obtained by comparing the magnetization with that of pure cobalt flakes. The magnetization and corresponding mass ratios of cobalt for the three samples are shown in Table 1.

Fig. 3(a) indicates that the real part of permeability (μ') for consolidated sample 1 decreases gradually with the increasing frequency. μ' of sample 2 exhibits completely different trend comparing with the former. It almost keeps constant value of 3 when

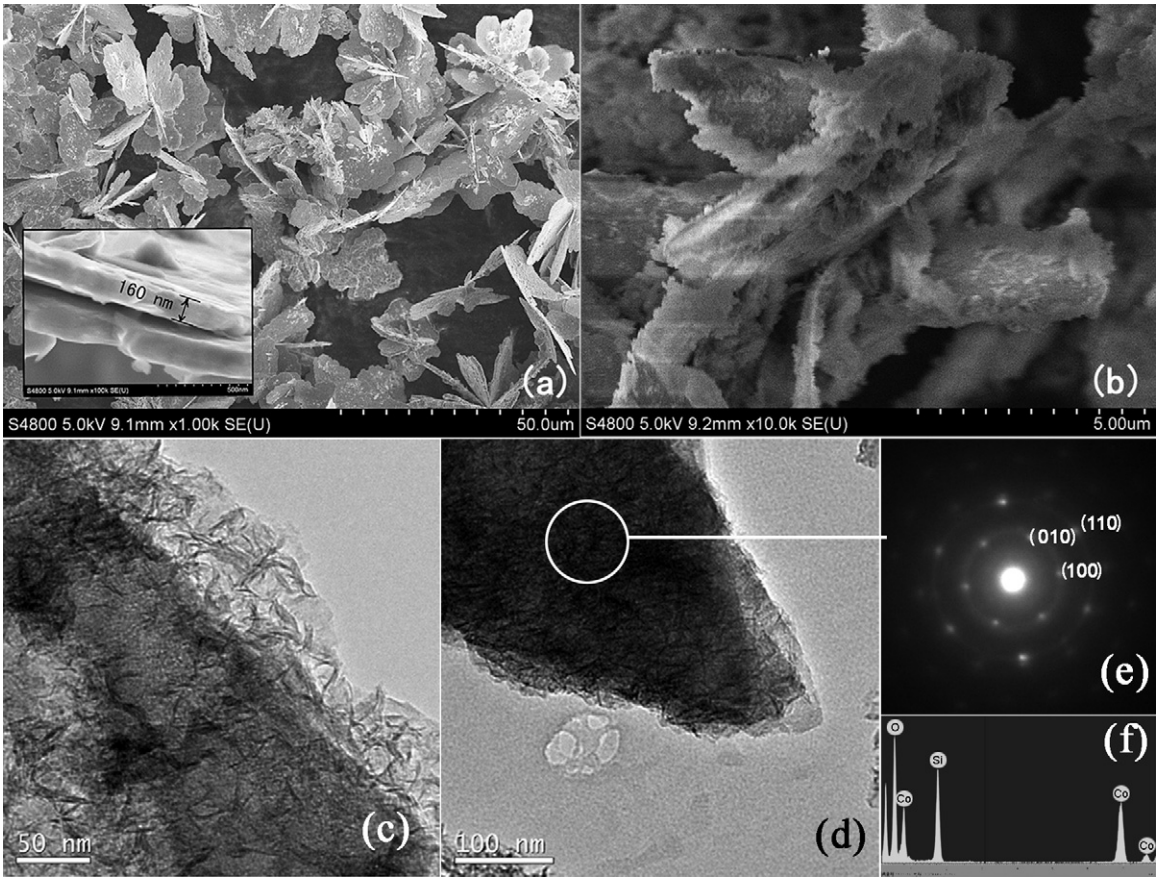

Fig. 2. SEM images of (a) sample 1, (b) sample 3, TEM images of (c) the edge of a silica coating flake, (d) the part of plane of a coated flake, (e) the SAED pattern in the white circle, and (f) the EDS pattern of sample 3.

Table 1
The magnetization (at 1 T) and corresponding mass ratio of cobalt for three samples.

	M at 1 T (emu/g)	Co mass ratio (%)
Sample 1	118	100
Sample 2	107	90
Sample 3	64	54

the frequency is lower than 3 GHz and rapidly drops down to about 0.6 when frequency increases to 7 GHz. A similar trend was also observed for μ' in sample 3 with lower initial value. The resonance frequencies of samples 2 and 3 are both about 4 GHz.

Fig. 3(b) indicates that the imaginary part of permeability (μ'') of sample 1 decreases gradually with the increasing frequency. The spectrum of sample 2 have a single peak at about 4 GHz from 0.1 to 10 GHz and a similar trend is also observed in sample 3. The inset shows the magnetic loss tangent for samples 2 and 3. It can be seen that the value of magnetic loss factors ($\tan\delta_m = \mu''/\mu'$) for samples 2 and 3 vary in the ranges of 0.15–1.33 and 0.15–0.78 over 1–10 GHz respectively.

The gradual decreasing of μ' for sample 1 in Fig. 3(a) can be ascribed to eddy current loss. According to the results of laminated Fe/SiO_2 composites, the eddy current plays a major role in total core energy loss at about $f > 100$ MHz [12] for the consolidated Fe flakes without any insulating coating. The eddy current loss (w_{es}) is shown by $w_e = kB^2t^2f^2/\rho$, where k is constant, B is the magnetic flux density, ρ is the resistivity, t is the sample thickness, and f is the frequency [18]. In this work, B is parallel to the plane of flakes; the direction of resulting eddy current is vertical to the plane. In the consolidated sample 1, due to the absence of an insulating barrier between neighboring flakes, some flakes are tightly connected and the thickness (t) is actually increased, which leads to strong eddy current in the lamination, and w_e rapidly increases with frequency increasing. After being coated with silica layer, each flake is separated by the silica coatings; the eddy current is effectively suppressed in the laminates. As a consequence, the value of μ' nearly keeps constant when frequency is lower than 3 GHz for consolidated samples 2 and 3.

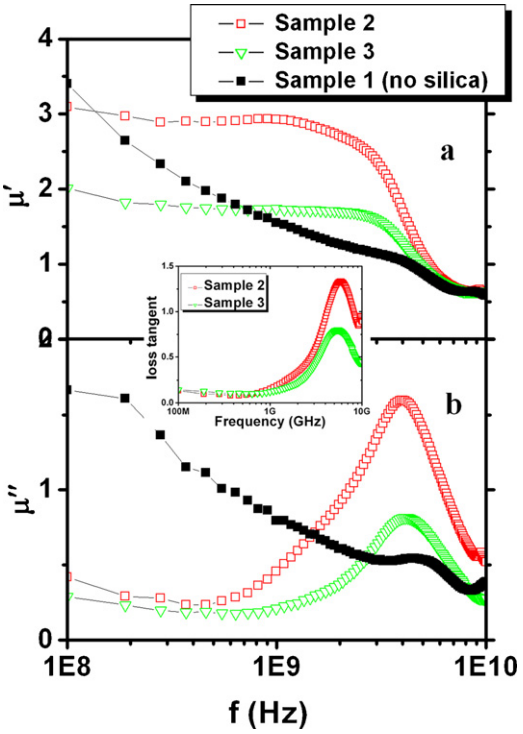

Fig. 3. Real part of permeability (μ') and imagery part of permeability (μ'') of consolidated samples 1, 2 and 3 vs frequency, the inset shows the magnetic loss tangent for samples 2 and 3.

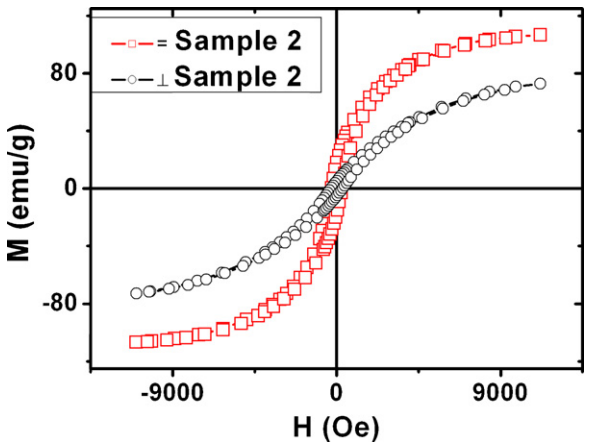

Fig. 4. Hysteresis loops in parallel and vertical directions of consolidated sample 2.

The single peak of μ'' at about 4 GHz for all coated samples indicates that there is the maximal magnetic loss. In general, magnetic loss originates mainly from hysteresis, domain wall resonance, natural ferromagnetic resonance and eddy current loss. The hysteresis loss is associated with irreversible magnetization and can be ignored in weak applied field. The domain wall resonance usually occurs in 1–100 MHz range. In this study, permeability measurements were carried out at a low microwave power (10 W) and a frequency range (0.1–10 GHz). At this point, domain wall resonance and hysteresis loss both can be excluded from this discussion. The eddy current loss cannot cause a resonance peak. Therefore, the single peak of μ'' at about 4 GHz should be caused by natural resonance.

The natural resonance frequency (f_r) of cobalt flakes is determined by the total effective anisotropy field (H_e). In this system, the H_e is determined by magnetocrystalline anisotropy field and demagnetizing field. In order to find the direction of H_e, we obtained the hysteresis loops in the parallel and vertical direction of the toroidal shaped sample plane by VSM.

Fig. 4 shows the hysteresis loops for consolidated sample 2 in two of the directions. The magnetization in parallel direction is larger than that in vertical direction when the applied field varied from 0 to 1.1 T, and it cannot reach the saturation status in both two directions. The coercivity is 266 Oe in parallel and 298 Oe in vertical direction. Obviously, the consolidated sample 2 is easy to be magnetized in the parallel direction. The direction of H_e should be nearly parallel to the plane of the compacted ring. The f_r can be simply calculated by: $f_r = (\gamma\sqrt{4\pi M_s H_e})/2\pi$ [22], where γ is the gyromagnetic factor (2.8 GHz/kOe), M_s is the saturation magnetization. $4\pi M_s = 4200$ Oe is obtained in hysteresis loop in parallel direction for sample 3 when $H = 1$ T. $H_e \approx H_c = 266$ Oe, the calculated f_r equals to 2.96 GHz. The value is lower than 4 GHz; it means that H_e is lager than H_c. The results of detailed fitting and calculation are provided, and the fitted value of H_e and other parameters are presented below.

The behavior of magnetization in high frequency magnetic field in the consolidated flakes can be described by the Landau–Lifshitz–Gilbert (L–L–G) equation:

$$\frac{d\vec{M}}{dt} = -\gamma(\vec{M}\times\vec{H}) + \frac{a}{M_s}\vec{M}\times\frac{d\vec{M}}{dt}, \quad (3)$$

where $\vec{M}$ is the magnetization, $\vec{H}$ is the total effective anisotropy field vector, γ is the gyromagnetic factor, α is the damping coefficient, and M_s is the saturation magnetization.

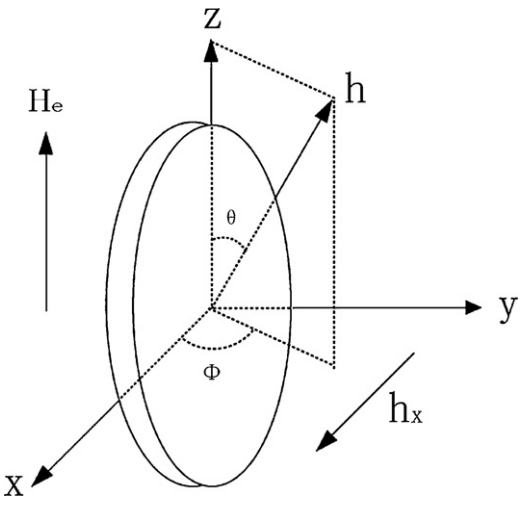

Fig. 5. The coordinate system in a cobalt flake.

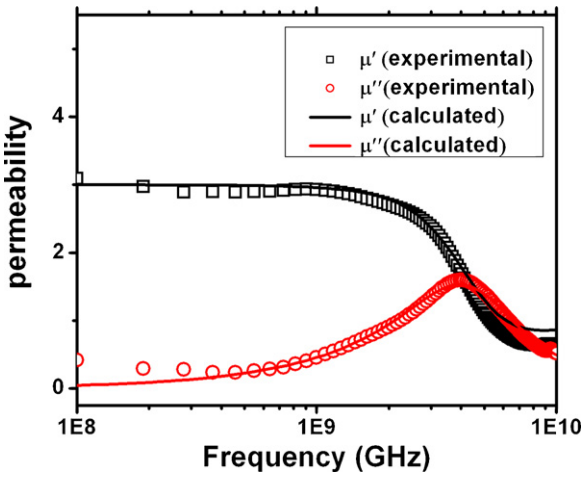

Fig. 6. The experimental and calculated complex permeability of sample 2.

When an ac field is applied in the plane of ring (a simplified diagram is shown in Fig. 5), the field and magnetization is given below:

$$\vec{M} = m_x, m_y, M_s + m_z, \tag{4}$$

$$\vec{H} = h_x, -4\pi m_y, H_e, \tag{5}$$

The microwave power is low, thus $|h| << |H_e|$ and $|m| << |M_s|$, complex permeability can be obtained by solving L–L–G equation:

$$\mu' = 1 + \frac{\omega_m(\omega_0+\omega_m)(\omega_r^2+\omega^2)+\alpha^2\omega^2\omega_m\omega_0}{[\omega_r^2-\omega^2(1+\alpha^2)]^2+\alpha^2\omega^2(2\omega_0+\omega_m)^2}, \tag{7}$$

$$\mu'' = \omega\omega_m\alpha\frac{(\omega_0+\omega_m)^2+\omega^2(1+\alpha^2)}{[\omega_r^2-\omega^2(1+\alpha^2)]^2+\alpha^2\omega^2(2\omega_0+\omega_m)^2}, \tag{8}$$

where $\omega_m = \gamma 4\pi M_s$, $\omega_0 = \gamma H_e$, and $\omega_r = \sqrt{\omega_0(\omega_0+\omega_m)}$. Fig. 6 shows the fitting results for sample 2, where $4\pi M_s$ is 4200 Oe, black and red solid line represent theoretical fitting curves of the μ' and μ'' respectively (For interpretation of the references to color in this text, the reader is referred to the web version of the article.). It is found that the experiment data (black square and red circle) are in good agreement with the fitting curves. The fitting results show that $\alpha = 0.72$ and $H_e = 466$ Oe. The total effective anisotropy field (H_e) is a resultant field of magnetocrystalline anisotropy field and demagnetizing field. According to Stoner–Wohfarth theory [23], the H_e derived from H_c carry a factor of 2. Therefore, it is expected that the effective field H_e is between H_c and $2H_c$. The calculated value of H_e equal to 1.7 H_c in parallel direction, it is surely in this range.

4. Conclusions

We successfully fabricated cobalt flakes coated with silica layers. Microwave measurements show a significant enhancement of μ' when frequency is lower than 3 GHz in coated samples, which is ascribed to the suppression of eddy current loss after silica coating. The resonance frequency for all coated samples is about 4 GHz. The single resonance peak of μ'' is assigned to be caused by the natural resonance.

Acknowledgements

The work is supported by the National Natural Science Foundation of China (Grant No. 11034004) and National Science Fund Distinguished Young Scholars (Grant 50925103).

References

[1] Y. Hayakawa, A. Makino, H. Fujimori, H.A. Inoue, J. Appl. Phys. 81 (1997) 3747.
[2] M.E. McHenry, M.A. Willard, H. Iwanabe, R.A. Sutton, Z. Turgut, A. Hsiao, D.E. Laughlin, Bull. Mater. Sci. 22 (1999) 495.
[3] T. Kasagi, T. Tsutaoka, K. Hatakeyama, IEEE Trans. Magn. 35 (1999) 3424.
[4] J. Moulin, Y. Champion, L.K. Varga, J.M. Greneche, F. Mazaleyrat, IEEE Trans. Magn. 38 (2002) 3015.
[5] T. Zhao, Q.F. Xiao, Z.D. Zhang, M. Dahlgren, R. Grossinger, K.H.J. Bushow, Appl. Phys. Lett. 75 (1999) 2298.
[6] Y.W. Zhao, T. Zhang, J.Q. Xiao, J. Appl. Phys. 93 (2003) 8014.
[7] Y.W. Zhao, C.Y. Ni, D. Kruczynski, X.K. Zhang, J.Q. Xiao, J. Phys. Chem. B 108 (2004) 3691.
[8] D.L. Zhao, Q. Lv, Z.M. Shen, J. Alloys Compd. 480 (2009) 634.
[9] T. Jahanbin, M. Hashim, K.A. Matori, S.B. Waje, J. Alloys Compd. 503 (2010) 111.
[10] L. Jia, J. Luo, H. Zhang, G. Xue, Y. Jing, J. Alloys Compd. 489 (2010) 162.
[11] X. Ni, J. Ma, J.G. Li, D.M. Jiao, J.J. Huang, X.D. Zhang, J. Alloys Compd. 468 (2009) 386.
[12] Y.W. Zhao, X.K. Zhang, J.Q. Xiao, Adv. Mater. 17 (2005) 915.
[13] B.S. Zhang, Y. Feng, J. Xiong, Y. Yang, X.H. Lu, IEEE Trans. Magn. 42 (2006) 1778.
[14] R.M. Walser, W. Win, P.M. Valanju, IEEE Trans. Magn. 34 (1998) 1390.
[15] Y.Q. Kang, M.S. Cao, J. Yuan, J. Alloys Compd. 495 (2010) 254.
[16] D.L. Zhao, X. Li, Z.M. Shen, J. Alloys Compd. 471 (2009) 457.
[17] A.H. Taghvaei, H. Shokrollahi, K. Janghorban, J. Alloys Compd. 481 (2009) 681.
[18] X.K. Zhang, T. Ekiert, K.M. Unruh, J. Appl. Phys. 99 (2006) 08M914.
[19] R. Ramprasad, P. Zurcher, M. Petras, M. Miller, J. Appl. Phys. 96 (2004) 519.
[20] J. Li, Y. Qin, X. Kou, J.J. Huang, Nanotechnology 15 (2004) 982.
[21] V.F. Puntes, D. Zanchet, C.K. Erdonmez, A.P. Alivisatos, P. Renaud, J. Am. Chem. Soc. 124 (2002) 12874.
[22] C. Kittel, Phys. Rev. 73 (1948) 155.
[23] S. Chikazumi, Physics of Ferromagnetism, Clarendon, Oxford, 1997.